Anisotropy and the inversion splitting in the $T_{1u} \otimes h_g$ Jahn - Teller system

1997 J. Phys.: Condens. Matter 9 7119

(http://iopscience.iop.org/0953-8984/9/34/006)

J. Phys.: Condens. Matter **9** (1997) 7119–7134. Printed in the UK PII: S0953-8984(97)78812-X

Anisotropy and the inversion splitting in the $T_{1u} \otimes h_g$ Jahn–Teller system

Y M Liu†, J L Dunn†, C A Bates† and V Z Polinger‡

† Physics Department, University of Nottingham, University Park, Nottingham NG7 2RD, UK§
‡ MSC Division, BYU–Hawaii Campus, Laie, Hawaii 96762-1294, USA

Received 21 October 1996, in final form 11 March 1997

Abstract. We present an analysis of the $T_{1u} \otimes h_g$ Jahn–Teller (JT) system in which both possible h-type quadratic terms are considered. It is well known that this results in pentagonal (D_{5d}) or trigonal (D_{3d}) minima on the potential energy surface, depending on the magnitudes of the coupling constants. Although the positions of the minima with quadratic couplings are known, the anisotropic effects which occur due to the lifting of the degeneracy of the h-vibrations by the quadratic coupling have not been studied before. Such effects have previously been found to be important in cubic systems. We investigate the nature of the minima by evaluating the curvature of the potential energy surface, and hence we determine the frequencies of the local vibrational modes in the strong-coupling limit as a function of the quadratic coupling strengths for the first time. We find that, in the linear coupling limit, the frequency of one of the e-modes at the minima tends to zero. This is as expected because, in this limit, the minimum-energy surface is a trough joining the D_{3d} and D_{5d} points.

A scale transformation method is then used, which allows the anisotropy effect to be incorporated into the states associated with the D_{5d} wells. States having the required icosahedral symmetry of the system as a whole are then written down in terms of the anisotropic states. Specific results will be given for the dependence of the inversion splitting on the anisotropy. The new states are of significance because they are necessary for the calculation of further properties of these systems, such as reduction factors. The system is also a possible model for the ground state of the C_{60}^{-} anion.

1. Introduction

Prior to the discovery of C_{60}, very little theoretical work had been done on JT effects in icosahedral (I_h) symmetry (the two notable exceptions being those of Khlopin *et al* [1] and Pooler [2]). The high symmetry of icosahedral systems opens many new exciting possibilities from a theoretical point of view, as the electronic and vibrational systems have threefold, fourfold and fivefold degeneracies (which can be labelled by the irreducible representations (IRs) T, G and H respectively of the I_h group). Orbital degeneracies above threefold are rare in other systems. The possible JT effects include the coupling of an orbital triplet to the fivefold degenerate vibrational modes (namely the $T \otimes h$ problem), the coupling of the fourfold degenerate orbital level to the fourfold and/or fivefold degenerate vibrations (i.e. $G \otimes (g + h)$ etc) and the coupling of a fivefold orbitally degenerate level to the fourfold and/or fivefold vibrational modes ($H \otimes (g + h)$ etc).

Molecular orbital calculations for C_{60} indicate that the unfilled orbital of lowest energy is of T_{1u} symmetry. Thus on doping the molecule with an impurity, one or more electrons

§ Please address correspondence to Nottingham.

0953-8984/97/347119+16$19.50

will occupy this T_{1u} orbital. The symmetries of the possible JT effects must occur in the direct product $T_1 \otimes T_1 = A_1 \oplus T_1 \oplus H$. The A_1 term is ignored as usual and the T_1 term is excluded because it changes sign under time reversal. Thus the ground state of the C_{60}^- anion is expected to exhibit a $T_{1u} \otimes h_g$ JT effect. It is this system which has received most attention in the literature.

A number of papers have been published which consider the linearly coupled $T_{1u} \otimes h_g$ JT system, in which the potential energy surface contains a trough of SO(3) symmetry. Auerbach *et al* [3] studied the problem starting from a weak-coupling basis. O'Brien [4], starting from a strong-coupling regime, used a parametrization of the five components of the h_g mode applicable to the higher SO(3) symmetry in order to simplify the problem. She was then able to obtain analytical and numerical results which cover all coupling strengths. The non-linear (i.e. warped) $T_{1u} \otimes h_g$ JT system has been studied in less detail. Ceulemans and Vanquickenborne [5] describe the effect of warping using spherical harmonic functions, and plot the warping potential in electronic space. O'Brien [4] also discusses how the energies obtained in the linear picture reduce to the icosahedral results when warping is imposed. When warping is included, there are found to be minima located at pentagonal (D_{5d}) and trigonal (D_{3d}) positions in Q-space, with saddle points of D_{2h} symmetry in between. If the warping effect is large, it is necessary to consider the wavefunctions in terms of linear combinations of states localized in the D_{5d} or D_{3d} minima in the potential energy surface, and not as perturbations on SO(3) states. Dunn and Bates [6] discussed JT effects in $T_{1u} \otimes h_g$ using such a model with two quadratic terms included in the vibronic Hamiltonian. A general form for the ground states was also given by Wang *et al* [7]. Both methods give results consistent with the predictions of O'Brien [4].

In linear coupling, the $T \otimes h$ system can be compared in some respects to that of the special case of the linear $T \otimes (e + t_2)$ JT system which occurs in cubic symmetry when the e- and t_2-modes have equal JT energies. Both cases are described by mathematically similar Hamiltonians, and in both cases the points of lowest energy on the potential energy surface form a two-dimensional trough. Also, if higher-order coupling terms are included in the vibronic Hamiltonians then the trough warps in both cases, giving distinct minima located at lower symmetry positions. However, although similar techniques can be used to study both systems, the positions of the wells and the detailed mathematics necessary to describe them are different in each case due to the differing point group symmetries. In addition, whereas in the cubic $T \otimes (e + t_2)$ JT system unequal coupling can be considered to be a warping mechanism, there is no analogue to this for $T_{1u} \otimes h_g$. Therefore the sign and magnitude of the second-order coupling constants are especially important in determining the properties of the minima in the quadratic $T_{1u} \otimes h_g$ JT system. A full discussion of the comparisons between the two systems with warping was given by Ceulemans and Vanquickenborne [5].

At the minima, the degeneracy of the vibrational frequency of the h_g modes will be lifted. Local modes of lower symmetries will exist, which have their own vibrational frequencies and so introduce anisotropy into the system. However, in previous publications on $T_{1u} \otimes h_g$ JT systems, this anisotropy has been ignored. The deviations of the anisotropic frequencies from the isotropic ones increase as the strengths of the quadratic couplings (and hence of the warping) increase. It is not known whether the effect will be significant for fullerene systems, as the magnitude of the deviation from SO(3) symmetry is expected to be small [4, 3]. However, it is important to calculate the magnitude of the anisotropy effect to determine whether its omission is reasonable, as well as from a theoretical point of view. Indeed, anisotropy is known to have significant effects in cubic systems ([8] and references therein). The changes in frequency of the local modes will alter the vibrational contributions to the vibronic states, which in turn will affect other important results such as the reduction

factors [9–11].

The approach of Dunn and Bates [6] will be developed further in this paper by incorporating anisotropy effects into the $T_{1u} \otimes h_g$ JT problem. We will examine how different values (sign and size) of the quadratic coupling constants and the local vibrational frequencies affect the nature of the minima, the associated vibronic states and their energies. We begin by presenting second-order perturbation calculations to determine the local vibrational frequencies in the strong-coupling lines using the method of Öpik and Pryce [12]. In so doing, we examine the shape of the minima and give the ranges of the quadratic coupling constants for which the wells are absolute minima. Vibronic states associated with the potential wells were obtained previously for the isotropic frequency case using a unitary shift transformation and energy minimization technique [6]. A scale transformation procedure will then be employed in addition to this shift transformation in order to incorporate the anisotropic frequencies into the states for the D_{5d} wells. Results for the D_{3d} minima are not given at this stage due to the additional complication of a repeated IR in the reduction of the frequencies to local modes.

As in the previous approach neglecting anisotropy, linear combinations of the states associated with the D_{5d} wells having the required icosahedral symmetry will then be taken using projection operator techniques. This is effectively allowing tunnelling between the wells to occur, and so automatically turns a static picture into one which is dynamic in character. Inversion (or tunnelling) splittings between the vibronic states will then be calculated and compared with the isotropic case. Results will be presented for the inversion splitting due to the tunnelling of the JT system between equivalent D_{5d} minima.

2. The vibronic Hamiltonian and local minima

As $h \otimes h = a \oplus t_1 \oplus t_2 \oplus 2g \oplus 2h$, the relevant quadratic terms for the $T_{1u} \otimes h_g$ JT systems are composed of two terms of repeating h-symmetry. The vibronic Hamiltonian $\mathcal{H}$ including quadratic terms has been given in [6]. Here, we rewrite $\mathcal{H}$ in the modified form

$$\mathcal{H} = \frac{1}{2}\sum_j \left[\frac{P_j^2}{\mu} + \mu\omega^2 Q_j^2\right] I + V_1 \sum_j Q_j C_j + V_2 \sum_j \{Q_h \otimes Q_h\}_j C_j + V_3 \sum_j \{Q_h \otimes Q_h\}'_j C_j \tag{2.1}$$

where V_1 is the linear coupling coefficient and V_2 and V_3 are the two independent quadratic coupling coefficients for the two h-terms (denoted here as unprimed and primed contributions). The sum j is taken over the five components of the h_g-mode (θ, ϵ, 4, 5 and 6) and I is the three-dimensional unit matrix. The C_j are Clebsch–Gordan (CG) matrices, which may be expressed in the form

$$C_\theta = \frac{1}{2}\sqrt{\frac{3}{5}}\begin{bmatrix} \phi^{-1} & 0 & 0 \\ 0 & -\phi & 0 \\ 0 & 0 & 1 \end{bmatrix} \qquad C_\epsilon = \frac{1}{2}\sqrt{\frac{1}{5}}\begin{bmatrix} \phi^2 & 0 & 0 \\ 0 & -\phi^2 & 0 \\ 0 & 0 & -\sqrt{5} \end{bmatrix}$$

$$C_4 = \sqrt{\frac{3}{10}}\begin{bmatrix} 0 & 0 & 0 \\ 0 & 0 & 1 \\ 0 & 1 & 0 \end{bmatrix} \qquad C_5 = \sqrt{\frac{3}{10}}\begin{bmatrix} 0 & 0 & 1 \\ 0 & 0 & 0 \\ 1 & 0 & 0 \end{bmatrix} \qquad C_6 = \sqrt{\frac{3}{10}}\begin{bmatrix} 0 & 1 & 0 \\ 1 & 0 & 0 \\ 0 & 0 & 0 \end{bmatrix} \tag{2.2}$$

with respect to electronic basis states x, y and z, where $\phi = \frac{1}{2}(1+\sqrt{5})$ is the golden mean. A general definition for quadratic terms is

$$\{Q_{\Gamma_1} \otimes Q_{\Gamma_2}\}_{i\Gamma\gamma} = \sum_{\gamma_1\gamma_2} Q_{\Gamma_1\gamma_1} Q_{\Gamma_2\gamma_2} \langle \Gamma_1\gamma_1\Gamma_2\gamma_2 \mid \Gamma\gamma\rangle_i \tag{2.3}$$

where the $\langle \Gamma_1\gamma_1\Gamma_2\gamma_2 \mid \Gamma\gamma\rangle_i$ are CG coefficients, which can be looked up from tables [13]. i is a multiplicity label added to distinguish between the different Γ in $\Gamma_1 \otimes \Gamma_2$. For our case, the contributions to the two types of quadratic term of repeating h-symmetries are thus found to be

$$\begin{aligned}\sum_j \{Q_h \otimes Q_h\}_j C_j \; &= \left[\sqrt{\frac{1}{2}}Q_\theta Q_\epsilon + \sqrt{\frac{3}{8}}(Q_4^2 - Q_5^2)\right]C_\theta \\ &+\sqrt{\frac{1}{8}}(Q_\theta^2 - Q_\epsilon^2 + Q_4^2 + Q_5^2 - 2Q_6^2)C_\epsilon + \sqrt{\frac{1}{2}}Q_4(\sqrt{3}Q_\theta + Q_\epsilon)C_4 \\ &+\sqrt{\frac{1}{2}}Q_5(-\sqrt{3}Q_\theta + Q_\epsilon)C_5 - \sqrt{2}Q_\epsilon Q_6 C_6 \end{aligned} \tag{2.4}$$

and

$$\begin{aligned}\sum_j \{Q_h \otimes Q_h\}'_j C_j = &\left[\sqrt{\frac{3}{8}}(Q_\theta^2 - Q_\epsilon^2) - \sqrt{\frac{1}{24}}(Q_4^2 + Q_5^2 - 2Q_6^2)\right]C_\theta \\ &-\left[\sqrt{\frac{3}{2}}Q_\theta Q_\epsilon - \sqrt{\frac{1}{8}}(Q_4^2 - Q_5^2)\right]C_\epsilon - \sqrt{\frac{1}{6}}[Q_4(Q_\theta - \sqrt{3}Q_\epsilon) + 2\sqrt{2}Q_5 Q_6]C_4 \\ &-\sqrt{\frac{1}{6}}[Q_5(Q_\theta + \sqrt{3}Q_\epsilon) + 2\sqrt{2}Q_4 Q_6]C_5 + \sqrt{\frac{2}{3}}[Q_\theta Q_6 - \sqrt{2}Q_4 Q_5]C_6. \end{aligned} \tag{2.5}$$

The quadratic terms in the vibronic Hamiltonian warp the potential energy surface, which would be a two-dimensional trough in the linear coupling case, giving extrema of pentagonal (D_{5d}) and trigonal (D_{3d}) symmetry [4, 14]. The splitting of the T_{1u} orbital at each of these extrema can be predicted easily using group theory. The decomposition of the IR T_{1u} of the icosahedral group to the lower point groups can be obtained from group character tables. Thus we find $T_{1u} \rightarrow A_{2u} + E_{1u}$ for the D_{5d} group and $T_{1u} \rightarrow A_{2u} + E_u$ for the D_{3d} group. The A_{2u} states have the lowest energy in both cases. We note that combinations of these lowest-energy states must be taken to produce ground states having the correct symmetry for the system as a whole (which is physically equivalent to allowing tunnelling between the minima).

The coordinates $Q_j^{(k)}$ for the D_{5d} and D_{3d} extrema were obtained in [6]. The electronic states associated with them, together with their energies, were also obtained by substituting the values of the extrema positions $Q_j^{(k)}$ into the potential energy matrix U (which can be obtained by simply ignoring the kinetic energy term in $\mathcal{H}$) and diagonalizing it. The six equivalent ground states for the minima of D_{5d} symmetry (each of symmetry A_{2u}) were labelled A–F, and the ten ground states for the D_{3d} minima were labelled a–j. The results obtained for the wells A and a are summarized in table 1. The energies of the E_u-states have also been given. The results have been defined in terms of the parameters

$$\beta = \frac{\sqrt{6}}{(5 - 4\sqrt{2}V_2')} \qquad \text{and} \qquad \gamma = \frac{\sqrt{2}}{(\sqrt{15} - 4\sqrt{2/3}V_3')} \tag{2.6}$$

where $V_i' = V_i/\mu\omega^2$ ($i = 2,\ 3$) and

$$K_1 = -\sqrt{\frac{\hbar}{2\mu\omega}}V_1. \tag{2.7}$$

The remaining states (and their energies) can be obtained by reference to tables I and II of [6].

Table 1. The coordinates $Q_j^{(k)}$ for one of the extrema points, the ground and excited states in the extremum together with the corresponding energies. In the table, the parameters β' and γ' are given by $\beta' = \beta V_1/\mu\omega^2$ and $\gamma' = \gamma V_1/\mu\omega^2$.

Symmetry group	Label	Coordinates $Q_\theta^{(k)}$, $Q_\epsilon^{(k)}$, $Q_4^{(k)}$, $Q_5^{(k)}$, $Q_6^{(k)}$	Electronic states	Energy
D_{5d}	A	$\beta'/\sqrt{2}, \beta'/\sqrt{6}, -\beta', 0, 0$	$\|A_{2u}\rangle = (\sqrt{5}\phi)^{-1/2}\|\phi y + z\rangle$	$E^{(I)}_{A_{2u}} = -\sqrt{\frac{2}{3}}\beta\frac{K_1^2}{\hbar\omega}$
			$\|E_{1u}\theta\rangle = \|x\rangle$	$E^{(I)}_{1u} = \frac{2}{3}(5-\sqrt{2}V_2')\beta^2\frac{K_1^2}{\hbar\omega}$
			$\|E_{1u}\epsilon\rangle = (\sqrt{5}\phi)^{-1/2}\|y - \phi z\rangle$	
D_{3d}	a	$-\gamma'/\sqrt{2}, \sqrt{3}\gamma'/\sqrt{2}, -\gamma', 0, 0,$	$\|A_{2u}\rangle = 3^{-1/2}\|\phi^{-1}y + \phi z\rangle$	$E^{(D)}_{A_{2u}} = -\sqrt{\frac{6}{5}}\gamma\frac{K_1^2}{\hbar\omega}$
			$\|E_u\theta\rangle = \|x\rangle$	$E^{(D)}_{E_u} = \frac{2}{5}(15-\sqrt{10}V_3')\gamma^2\frac{K_1^2}{\hbar\omega}$
			$\|E_u\epsilon\rangle = 3^{-1/2}\|-\phi y + \phi^{-1}z\rangle$	

Using the expressions for the energies of the wells given in table 1, we can find the values of the quadratic coupling constants for which each type of extremum becomes an absolute minimum. One restriction follows immediately from the requirement that the JT system should remain stable. The other restriction is found by comparing the energies of the pentagonal and trigonal wells [6]. Thus we find that

$$\frac{3}{\sqrt{5}}V_2' > V_3' > -\frac{3}{8}\sqrt{10} \qquad \text{and} \qquad V_2' < \frac{5}{8}\sqrt{2} \tag{2.8}$$

for the pentagonal wells to be absolute minima. For trigonal extrema to be absolute minima, we find

$$\frac{\sqrt{5}}{3}V_3' > V_2' > -\frac{5}{8}\sqrt{2} \qquad \text{and} \qquad V_3' < \frac{3}{8}\sqrt{10}. \tag{2.9}$$

Along the line $\sqrt{5}V_3' = 3V_2'$, the pentagonal and trigonal points coexist, and together with the dihedral (D_{2h}) points form a two-dimensional trough. Figure 1 shows the ranges of values for the scaled quadratic coupling coefficients V_2' and V_3' for which D_{3d} and D_{5d} minima exist. Ceulemans [14] has pointed out that a tensor of tenth order (including also the twofold orbital part) is needed for the D_{2h} extrema to become absolute minima. This means that quartic coupling terms $h \otimes h \otimes h \otimes h$ would need to be included in the vibronic Hamiltonian. This will not be considered further in this paper.

3. Local vibrational frequencies

An important property of the $T_{1u} \otimes h_g$ system with quadratic coupling is the frequencies of the oscillators located in the minima. Symmetry analysis shows that, at the pentagonal extrema, the vibrational modes of h_g-symmetry will be reduced to $a_{1g} + e_{1g} + e_{2g}$, while at the trigonal extrema they will be reduced to $a_{1g} + 2e_g$. Thus the fivefold degeneracy of the h_g modes is lifted in both cases. The values of the frequencies may be derived using the method of Öpik and Pryce [12]. This involves expanding the potential energy U as a power series about the minimum at the point $Q_j^{(k)}$ to give

$$U(q) = U(Q^{(k)}) + U_1(q) + U_2(q) \tag{3.1}$$

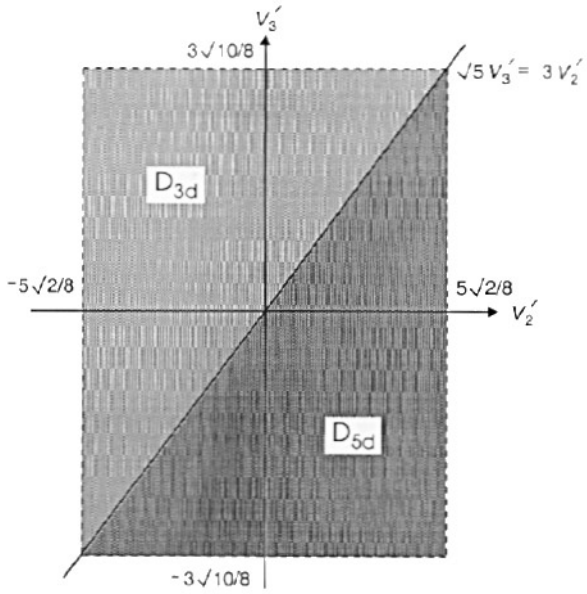

Figure 1. The domains of existence of the absolute minima of D_{5d}, D_{3d} and D_{2h} symmetries.

with

$$U_1(q) = \sum_{\Gamma\gamma} \left(\frac{\partial U}{\partial Q_{\Gamma\gamma}} \right)_{Q^{(k)}} q_{\Gamma\gamma} \qquad U_2(q) = \frac{1}{2} \sum_{\Gamma_1\gamma_1} \sum_{\Gamma_2\gamma_2} \left(\frac{\partial^2 U}{\partial Q_{\Gamma_1\gamma_1} \partial Q_{\Gamma_2\gamma_2}} \right)_{Q^{(k)}} q_{\Gamma_1\gamma_1} q_{\Gamma_2\gamma_2} \tag{3.2}$$

where $q_{\Gamma\gamma} = Q_{\Gamma\gamma} - Q_{\Gamma\gamma}^{(k)}$ are the nuclear displacements from the extrema.

The eigenstates and energies of the matrix $U(Q^{(k)})$ are known from the determination of the minima, and $U_1(q)$ and $U_2(q)$ treated as perturbations. Thus the eigenvalues of $U(q)$ up to second order are

$$E(q) = E_0(Q^{(k)}) + A_0^{\dagger} U_2 A_0 + \sum_{i \neq 0} \frac{|A_i^{\dagger} U_1 A_0|^2}{E_0(Q^{(k)}) - E_i(Q^{(k)})} \tag{3.3}$$

where the A_i and $E_i(Q^{(k)})$ are the eigenvectors and eigenvalues respectively of the matrix $U(Q^{(k)})$ and the sum i is taken over the excited orbital states. The term linear in $q_{\Gamma\gamma}$ is absent since, at the point $Q^{(k)}$, the function is at an extremum. Thus the expression (3.3) is a bilinear form of the displacements $q_{\Gamma\gamma}$. It can therefore be expressed in the matrix form

$$E(q) = E_0(Q^{(k)}) + \tfrac{1}{2}(q_{\Gamma_1\gamma_1} q_{\Gamma_1\gamma_2} \ldots) M \begin{pmatrix} q_{\Gamma_1\gamma_1} \\ q_{\Gamma_1\gamma_2} \\ \cdot \\ \cdot \\ \cdot \end{pmatrix} \tag{3.4}$$

where

$$M = \begin{pmatrix} \frac{\partial^2 E(q)}{\partial q_{\Gamma_1\gamma_1}^2} & \frac{\partial^2 E(q)}{\partial q_{\Gamma_1\gamma_1} \partial q_{\Gamma_1\gamma_2}} & \cdots \\ \frac{\partial^2 E(q)}{\partial q_{\Gamma_1\gamma_2} \partial q_{\Gamma_1\gamma_1}} & \frac{\partial^2 E(q)}{\partial q_{\Gamma_1\gamma_2}^2} & \cdots \\ \cdots & \cdots & \cdots \end{pmatrix}. \tag{3.5}$$

The new vibrational frequencies ω_Γ in the neighbourhood of the extrema can be obtained by diagonalizing the matrix M. Table 2 gives the resultant calculated frequencies ω_Γ of the local normal modes for both the pentagonal and trigonal wells in terms of λ_Γ^2, where $\lambda_\Gamma = \omega_\Gamma/\omega$. λ_1 and λ_2 are the roots of the quadratic equation $a\lambda^2 + b\lambda + c = 0$, where

$$a = -15 + 2\sqrt{10}V_3'$$
$$b = 135 - 90\sqrt{2}V_2' - 54V_2'^2 + 48\sqrt{10}V_3' - 118V_3'^2 + 60\sqrt{5}V_2'V_3'$$
$$c = \frac{3\sqrt{2}}{5}(-675 - 540\sqrt{2}V_2' - 90V_2'^2 + 90\sqrt{10}V_3' + 50V_3'^2 + 144\sqrt{5}V_2'V_3')(\sqrt{5}V_3' - 3V_2'). \tag{3.6}$$

It is interesting to note that, for both types of extremum, the frequencies of the a_{1g}-modes are only dependent upon one of the quadratic coupling coefficients (that is, on V_2' at the D_{5d} extrema and on V_3' at the D_{3d} extrema) but that the E-type frequencies depend on both V_2' and V_3'. Also, it is a simple matter to show analytically that the values of the frequencies given in table 2 are all positive within the regions of quadratic coupling for which the corresponding extrema are minima, as would be expected. We can also determine the maximum values of the frequencies allowed for the extrema to remain minima. For example, we have $\lambda_{a_{1g}} < 1.4$, $\lambda_{e_{1g}} < 1.3$ and $\lambda_{e_{2g}} < 1.4$ for the D_{5d} extrema to be absolute minima.

Table 2. The local frequencies in the D_{5d} and D_{3d} minima.

Symmetry group	Γ	Local vibrational frequency parameter λ_Γ^2 $(= \omega_\Gamma^2/\omega^2)$
D_{5d}	a_{1g}	$1 - \frac{4}{5}\sqrt{2}V_2'$
	e_{1g}	$\frac{1}{5}\frac{(3V_2' - \sqrt{5}V_3')(15\sqrt{2} - 18V_2' + 2\sqrt{5}V_3')}{5 - 2\sqrt{2}V_2'}$
	e_{2g}	$1 + \frac{\sqrt{2}}{5}V_2' + \sqrt{\frac{2}{5}}V_3'$
D_{3d}	a_{1g}	$1 - \frac{4}{15}\sqrt{10}V_3'$
	e_g	$\lambda_1/9$
	e_g'	$\lambda_2/9$

It can be seen that when $V_2' = V_3' = 0$, $\lambda_{a_{1g}} = \lambda_{e_{2g}} = 1$ for the D_{5d} minima, and $\lambda_{a_{1g}} = \lambda_{e_g} = 1$ for D_{3d}, but that $\lambda_{e_{1g}}$ (for D_{5d}) and e_g (for D_{3d}) tend to zero. This correctly represents the case in which the minimum potential energy surface consists of a two-dimensional trough, rather than distinct wells. It was necessary to take the calculations to second order in perturbation theory in order to obtain this result: to first order, all the λ tend to unity, which is equivalent to assuming there are isotropic wells.

4. The scale transformation for pentagonal wells

In our previous work for the isotropic case [6], the states in the wells were obtained initially by applying a unitary shift transformation U to displace the origins of coordinates. This will be called U_d here. The parameters in U_d were then determined by minimizing the energy of the predicted states. States in undisplaced coordinates were then obtained by multiplying

the states in each well k by the operator $U_d^{(k)}$, given by

$$U_d^{(k)} = \exp\left\{ -\frac{\mathrm{i}}{\hbar} \sum_j Q_j^{(k)} P_j \right\}. \tag{4.1}$$

This is equivalent to U_d after substitution of the values of Q_j appropriate for well k. Linear combinations of such states are later required in order to construct vibronic states of the system as a whole which have the required icosahedral symmetry. However, this method only incorporates the positions of the wells, and does not take into account the shapes of the minima. As shown above, when quadratic coupling is included, the wells are anisotropic, so this is an important omission. The anisotropy effect in the strong-coupling limit has been included in the states for cubic systems by treating the collective displacements Q_i at the minima as dynamic variables (see the discussion in [15] and references therein). However, the approach is not correct for finite couplings. Also, it is not an operator approach, so cannot be used in conjunction with the unitary transformation method. Hence the many advantages of this method are lost.

Very recently, a new procedure was used in order to incorporate anisotropy into the cubic T $\otimes$ t JT system [8]. A scale transformation U_s was applied to the Hamiltonian in addition to U_d. The shift transformation determines the positions of the minima, and the scale transformation determines the shape of the minima. The shift transformation parameters α were determined by minimizing the energy as before, and the parameters λ in the scale transformation were determined by minimization of the energy to second order in perturbation theory. The effect of this is to incorporate anisotropy formally into the theory without the need of any prior knowledge of its effects. It was also shown to produce results consistent with those of the Öpik–Pryce method [12] in the strong-coupling limit.

Unfortunately, the scale transformation procedure as applied to T $\otimes$ t cannot be applied directly to the problem under consideration here due to the added complication that the wells are necessarily generated by the quadratic coupling. Also it cannot be applied to cases containing repeated IRs in the reduction of the frequencies at the minima, as occurs for the D_{3d} minima (as the required matrices are not known). However, a modified procedure can be adopted to obtain strong-coupling results for the pentagonal (D_{5d}) extrema. Rather than fixing values for the scale transformation parameters λ by energy minimization, the λ can be replaced by the frequencies obtained using the Öpik–Pryce procedure. The scale transformation can then be applied directly to the states as in the T$\otimes$t case. Thus, proceeding with the pentagonal (D_{5d}) wells, we define a scale transformation for well k to be

$$U_s^{(k)} = \exp\left\{ \frac{\mathrm{i}}{\hbar} \sum_{ij} A_{ij}^{(k)} (Q_i P_j + P_j Q_i) \right\} \tag{4.2}$$

where the matrix elements $A_{ij}^{(k)}$ are defined by the matrix

$$A^{(k)} = \tfrac{1}{4} S_k^{\dagger} \begin{pmatrix} \ln\lambda_{a_{1g}} & 0 & 0 & 0 & 0 \\ 0 & \ln\lambda_{e_{1g}} & 0 & 0 & 0 \\ 0 & 0 & \ln\lambda_{e_{1g}} & 0 & 0 \\ 0 & 0 & 0 & \ln\lambda_{e_{2g}} & 0 \\ 0 & 0 & 0 & 0 & \ln\lambda_{e_{2g}} \end{pmatrix} S_k. \tag{4.3}$$

S_k is an as yet unknown unitary matrix which reduces the h_g modes of the I_h group to local modes of a_{1g}, e_{1g} and e_{2g} symmetries of the D_{5d} group for well k. It can be proved easily that the effect of the scale transformation on the ground vibrational states is to alter the h_g-mode frequency ω to a local mode frequency $\omega_\Gamma = \lambda_\Gamma \omega$ (as given in table 2). In principle, it would be possible to obtain the S_k by diagonalizing the matrix M in (3.5). However,

the inclusion of the quadratic terms in the vibronic Hamiltonian makes this process very difficult to execute. Therefore, we turn to symmetry considerations to simplify the problem.

When the fivefold degeneracy of the h_g-modes is lifted by the quadratic terms, h_g is reducible. Therefore S_k must be a unitary matrix which reduces reducible matrices into irreducible matrices belonging to the D_{5d} subgroup of I_h. This may be carried out by the traditional method of projection operator techniques but a simple alternative is to use the so-called eigenfunction method [16]. Details of this method are given in the appendix together with the results for the six matrices S_k for the D_{5d} minima.

The effect of the scale transformation is that the unitary transformation used to multiply the wells in [6] is replaced by the product operator $U_k = U_d^{(k)} U_s^{(k)}$. The states in the wells are thus written in the form

$$|\psi_k\rangle = U_k|\phi_k; 0\rangle = U_d^{(k)} U_s^{(k)}|\phi_k; 0\rangle \equiv |\phi_k'; 0\rangle. \tag{4.4}$$

The new overlap integral between the ground state vibrational wavefunctions localized in any two wells j and k becomes

$$S_I = \langle 0|U_j^\dagger U_k|0\rangle = \left\{ \frac{\lambda_{e_{1g}} \lambda_{e_{2g}} \nu}{[3\lambda_{a_{1g}} + \lambda_{e_{1g}} + \lambda_{e_{2g}}][2\lambda_{e_{1g}} + (3+\sqrt{5})\lambda_{e_{2g}}][(3+\sqrt{5})\lambda_{e_{1g}} + 2\lambda_{e_{2g}}]} \right\}^{1/2}$$
$$\times 10\sqrt{5}\phi \exp\left\{ -5\sqrt{6}\nu\beta \left(\frac{E_{JT}}{\hbar\omega} \right) \right\} \tag{4.5}$$

where

$$\nu = \frac{\lambda_{a_{1g}} \lambda_{e_{1g}} \lambda_{e_{2g}}}{\lambda_{a_{1g}}(\lambda_{e_{1g}} + \lambda_{e_{2g}}) + 3\lambda_{e_{1g}} \lambda_{e_{2g}}} \tag{4.6}$$

and where $E_{JT} = -E_{a_{2u}}^{(I)}$ (table 1) is the magnitude of the JT energy for pentagonal wells.

In the limit when $\lambda_{a_{1g}} = \lambda_{e_{1g}} = \lambda_{e_{2g}} = 1$, it can be seen that $U_s = 1$. In this case, the unitary transformation U_k reduces to the shift transformation used previously, and S_I becomes

$$S_I = \exp\{-\sqrt{6}\beta E_{JT}/\hbar\omega\} \tag{4.7}$$

as obtained in [6]. It is interesting to note that in the isotropic limit $V_2' = V_3' = 0$ (and hence $\lambda_{a_{1g}} = \lambda_{e_{2g}} = 1$ and $\lambda_{e_{1g}} = 0$), $S_I = 0$. This is because there are no longer distinct wells, but a trough. The original method, involving a unitary shift transformation only, does not reproduce the correct isotropic limit as the method intrinsically assumes the existence of wells.

5. The inversion splitting

The vibrational states localized in the D_{5d} or D_{3d} wells are good eigenstates of the system in the infinite-coupling limit. However, for finite coupling, the barrier height between the wells is not infinite and the system is able to tunnel from one well to another. The degeneracy of the states in the infinite-coupling limit will be partially or completely lifted by this tunnelling and the vibronic states will have full icosahedral symmetry. The vibronic states associated with the D_{5d} wells have T_{1u} and T_{2u} symmetries. They may be obtained using projection operators as described in [6] for the isotropic case. Consequently, the states are written in the same form as in [6] but taking the new definitions of the $|\psi_k\rangle$ from (4.4). Thus the x-components of the states are written as

$$|T_{1ux}^I\rangle = N_{T_{1u}}^I [\phi^{-1}(|C'; 0\rangle + |D'; 0\rangle) + |E'; 0\rangle - |F'; 0\rangle]$$
$$|T_{2ux}^I\rangle = N_{T_{2u}}^I [|C'; 0\rangle + |D'; 0\rangle - \phi^{-1}(|E'; 0\rangle - |F'; 0\rangle)] \tag{5.1}$$

with normalization factors

$$N^I_{T_{1u}} = [10(1+S_I)]^{-1/2} \qquad N^I_{T_{2u}} = [10(1-S_I)]^{-1/2}. \tag{5.2}$$

The y- and z-components can be found in [6].

The inversion splitting δ between the first excited vibronic state $|T^I_{2ui}\rangle$ and the ground vibronic state $|T^I_{1ui}\rangle$ is given by

$$\delta = \langle T^I_{2ui}|\mathcal{H}|T^I_{2ui}\rangle - \langle T^I_{1ui}|\mathcal{H}|T^I_{1ui}\rangle = \frac{2(S_I H_{11} + \sqrt{5}H_{12})}{1-S_I^2} \tag{5.3}$$

where $H_{11} = \langle\psi_k|\mathcal{H}|\psi_k\rangle$ and $H_{12} = \langle\psi_A|\mathcal{H}|\psi_B\rangle$, for example. (The matrix element between any two different wells is $\pm H_{12}$.) S_I is the phonon overlap given by (4.5). We note that the definitions of H_{11} and H_{12} used here are different to those given in [6], where the states ψ_k were not normalized and orbital overlap factors of $\sqrt{5}\phi$ and $-\phi$ were not included in the definitions of H_{11} and H_{12} respectively.

After evaluation of the new matrix elements, we find that

$$\begin{aligned} H_{11} = -E_{JT} + \frac{1}{4}\hbar\omega\Bigg[&\lambda_{a_{1g}} + 2\lambda_{e_{1g}} + 2\lambda_{e_{2g}} + \frac{1}{\lambda_{a_{1g}}}\left(1 - \frac{4}{5}\sqrt{2}V_2'\right) \\ &+ \frac{2}{\lambda_{e_{1g}}}\left[1 + \frac{1}{5}\left(\sqrt{2}V_2' - \sqrt{10}V_3'\right)\right] + \frac{2}{\lambda_{e_{2g}}}\left[1 + \frac{1}{5}(\sqrt{2}V_2' + \sqrt{10}V_3')\right]\Bigg] \end{aligned} \tag{5.4}$$

and

$$\begin{aligned} H_{12} = -\frac{S_I}{\sqrt{5}}\Bigg[&-\frac{5}{\sqrt{6}}\lambda^2_{a_{1g}}\beta E_{JT} + \frac{1}{2}\hbar\omega(\lambda_{a_{1g}} + 2\lambda_{e_{1g}} + 2\lambda_{e_{2g}}) \\ &-E_{JT}[f_1(\lambda)V_2' + f_2(\lambda)V_3' + f_3(\lambda)] \\ &-\hbar\omega[f_4(\lambda)V_2' + f_5(\lambda)V_3' + f_6(\lambda)]\Bigg] \end{aligned} \tag{5.5}$$

where

$$f_1(\lambda) = -\frac{5}{\sqrt{3}}\frac{\lambda^2_{a_{1g}}\beta}{g_1(\lambda)^2}(\lambda_{e_{2g}} - \lambda_{e_{1g}}(2-\sqrt{6}))(\lambda_{e_{2g}} - \lambda_{e_{1g}}(2+\sqrt{6}))$$

$$f_2(\lambda) = \sqrt{\frac{5}{3}}\frac{\lambda^2_{a_{1g}}\beta}{g_1(\lambda)^2}(3\lambda_{e_{2g}} + \lambda_{e_{1g}}(2+\sqrt{10}))(3\lambda_{e_{2g}} + \lambda_{e_{1g}}(2-\sqrt{10}))$$

$$\begin{aligned} f_3(\lambda) = -\frac{5\beta\lambda^2_{a_{1g}}}{\sqrt{6}g_1(\lambda)^2}&[(\lambda_{e_{1g}} + \lambda_{e_{2g}})^2 + (3+\lambda^2_{a_{1g}})(\lambda^2_{e_{1g}} + \lambda^2_{e_{2g}}) - 6\lambda^2_{e_{1g}}\lambda^2_{e_{2g}} \\ &+2\lambda_{a_{1g}}\lambda_{e_{1g}}\lambda_{e_{2g}}(\lambda_{a_{1g}} + 3\lambda_{e_{1g}} + 3\lambda_{e_{2g}})] + \frac{2}{g_1(\lambda)}\lambda_{a_{1g}}(\lambda_{e_{1g}} + 4\lambda_{e_{2g}}) \end{aligned}$$

$$\begin{aligned} f_4(\lambda) = \frac{\sqrt{2}}{4g_1(\lambda)}&(-\lambda_{a_{1g}} + 2\lambda_{e_{1g}} - \lambda_{e_{2g}}) \\ &+\frac{\sqrt{2}}{g_2(\lambda)}[\lambda^2_{e_{1g}} + 2\lambda_{e_{2g}}(5\lambda_{e_{1g}} + 2\lambda_{e_{2g}}) - 3\lambda_{a_{1g}}(4\lambda_{e_{1g}} + \lambda_{e_{2g}})] \end{aligned}$$

$$f_5(\lambda) = -\frac{3\sqrt{10}}{20g_1(\lambda)}(\lambda_{a_{1g}} + 2\lambda_{e_{1g}} - 3\lambda_{e_{2g}}) - \frac{\sqrt{10}}{g_2(\lambda)}[\lambda^2_{e_{1g}} + \lambda_{e_{2g}}(2\lambda_{e_{1g}} - 3\lambda_{a_{1g}})]$$

$$f_6(\lambda) = \frac{1}{4g_1(\lambda)}[\lambda_{a_{1g}}(\lambda^2_{e_{1g}} + \lambda^2_{e_{2g}} - 2) + (\lambda_{e_{1g}} + \lambda_{e_{2g}})(\lambda^2_{a_{1g}} + 3\lambda_{e_{1g}}\lambda_{e_{2g}} - 4)]$$

$$+\frac{1}{g_2(\lambda)}\{3\lambda_{a_{1g}}^2(\lambda_{e_{1g}}^2+\lambda_{e_{2g}}^2+3\lambda_{e_{1g}}\lambda_{e_{2g}})$$
$$+3\lambda_{a_{1g}}[2\lambda_{e_{1g}}^3+\lambda_{e_{1g}}(3\lambda_{e_{2g}}^2-5)+\lambda_{e_{2g}}(3\lambda_{e_{1g}}^2+2\lambda_{e_{2g}}^2-5)]$$
$$+\lambda_{e_{1g}}^3(3\lambda_{e_{1g}}+8\lambda_{e_{2g}})+2\lambda_{e_{1g}}^2(4\lambda_{e_{2g}}^2-5)+\lambda_{e_{1g}}\lambda_{e_{2g}}(8\lambda_{e_{2g}}^2-25)$$
$$+\lambda_{e_{2g}}^2(3\lambda_{e_{2g}}^2-10)\} \tag{5.6}$$

and where

$$g_1(\lambda)=\lambda_{a_{1g}}(\lambda_{e_{1g}}+\lambda_{e_{2g}})+3\lambda_{e_{1g}}\lambda_{e_{2g}}$$
$$g_2(\lambda)=(3\lambda_{a_{1g}}+\lambda_{e_{1g}}+\lambda_{e_{2g}})(2\lambda_{e_{2g}}+(3-\sqrt{5})\lambda_{e_{1g}})(2\lambda_{e_{2g}}+(3+\sqrt{5})\lambda_{e_{1g}}). \tag{5.7}$$

The value of H_{11} is equivalent to that obtained in [6] when all of the $\lambda = 1$ (noting that the definitions of their K_i ($i = 2, 3$) should be multiplied by $(K_1/\hbar\omega)^2$).

The inversion splitting can thus be expressed as

$$\delta=\frac{2S_I}{1-S_I^2}\left\{E_{JT}[f_1(\lambda)V_2'+f_2(\lambda)V_3'+f_3(\lambda)]\right.$$
$$\left.+\hbar\omega\left[\frac{1}{4\lambda_{e_{1g}}}(5-\lambda_{a_{1g}}^2-2\lambda_{e_{1g}}^2-2\lambda_{e_{2g}}^2)+f_4(\lambda)V_2'+f_5(\lambda)V_3'+f_6(\lambda)\right]\right\}. \tag{5.8}$$

It can be seen that δ depends on the JT energy, $\hbar\omega$ and the quadratic coupling constants V_2' and V_3'. The term involving $\hbar\omega$ arises from the complicated nature of the states in the wells from second-order perturbation theory. However, the contribution of this term to δ is small, especially in strong coupling. Also, we note that δ is positive, showing that the ground vibronic state has the same transformation properties as the original electronic term from which it was derived.

In figure 2, we compare the calculated values of δ as a function of $K_1/\hbar\omega$ using the results for the unitary shift transformation alone (as in [6]) and those obtained here using the anisotropic states. Results have been presented for $V_2' = V_3' = 0.01K_1/\hbar\omega$. These values are chosen as they ensures these extrema are indeed wells, and also keep the quadratic couplings much less than the linear coupling. It can be seen that the anisotropy strongly influences the magnitude of the tunnelling splitting, even in the strong-coupling region, with the inversion splitting always being significantly larger than the result obtained neglecting anisotropy. It can be seen that δ does not tend to unity in weak coupling (as in the isotropic case) because the quadratic coupling also tends to zero in this limit, so that the system is in the region with a trough of minimum energy. Hence the inversion level should be a rotational quantum for a two-dimensional trough in Q-space above the ground state, and not a vibrational quantum as in the isotropic results.

It is interesting to study the dependence of δ on the JT energy and on the barrier height h_B as a function of the distance d_M between any two of the D_{5d} minima in Q-space. The barrier height h_B can be defined as the difference between the energy of the D_{2h} saddle points and the D_{5d} minima. Using the results given in table 1 and the expression (3.9) in [6], we obtain

$$h_B=\frac{3\sqrt{5}}{40}\frac{(3V_2'-\sqrt{5}V_3')(3\sqrt{10}+8V_3')}{(5-V_2'^2-3V_3'^2)}E_{JT}. \tag{5.9}$$

The parameter d_M may be calculated from the values of the coordinates of the minima $Q_j^{(k)}$, with the result that $d_M = 2\beta|V_1|/\mu\omega^2$.

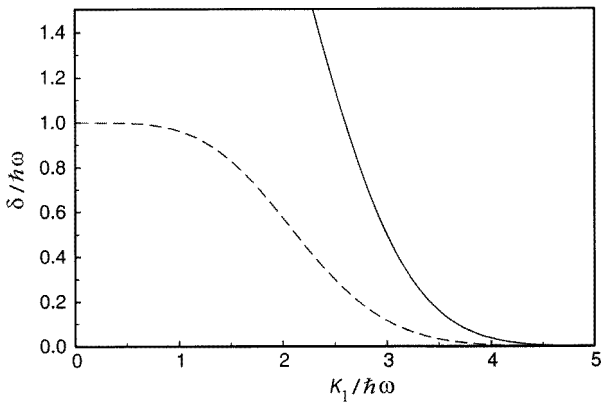

Figure 2. A comparison of the inversion splitting as a function of $K_1/\hbar\omega$ with anisotropy included (with $V_2' = -V_3' = 0.01K_1/\hbar\omega$) (solid line) and the isotropic case for which $V_2' = V_3' = 0$ (dashed line).

Figure 3 shows the variation of δ with barrier height for three fixed values of the JT energy. We see that δ is reduced in magnitude drastically when the barrier height h_B increases. The curves are only meaningful up to the maximum barrier height h_{Bmax} possible within the D_{5d} minimum domain, which can be calculated using (5.9). Thus, in figure 3, we have ended the curves at $h_{Bmax} = 0.4\hbar\omega$ for $E_{JT} = \hbar\omega$, $h_{Bmax} = 0.81\hbar\omega$ for $E_{JT} = 2\hbar\omega$ and $h_{Bmax} = 1.22\hbar\omega$ for $E_{JT} = 3\hbar\omega$. When h_B approaches zero, the values of δ will again tend to the rotational energy of the JT system rotating along a two-dimensional trough.

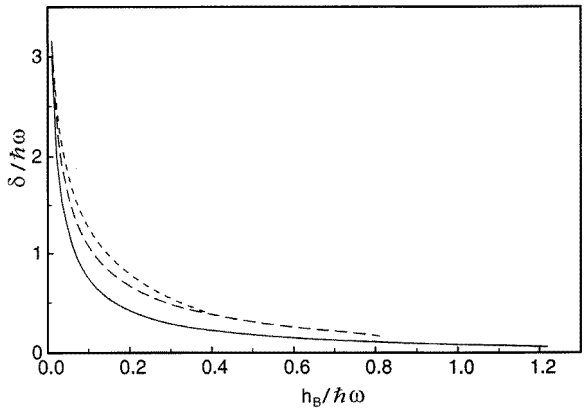

Figure 3. The inversion splitting as a function of the barrier height h_B for $E_{JT} = 3\hbar\omega$ (solid line), $2\hbar\omega$ (long-dashed line) and $\hbar\omega$ (short-dashed line). The separation between the minima is $d_M = \sqrt{\frac{8}{5}}|V_1|/\mu\omega^2$.

Figure 4 shows a plot of δ as a function of E_{JT} for fixed barrier heights. The curves start at different points corresponding to the minimum allowed value of the JT energy for that particular barrier height. This arises because if the barrier is not high enough or the JT coupling is not so strong we have only hindered rotation along the two-dimensional trough. It may be seen that δ decreases smoothly when E_{JT} increases with very strong coupling.

The criterion for tunnelling to occur is that $\overline{h}\omega_{e_g}$ should be less than the barrier height. In order that this condition is satisfied, calculations show that $E_{JT} > 5.5\overline{h}\omega$ for $h_B = 0.4\overline{h}\omega$, $E_{JT} > 3.2\overline{h}\omega$ for $h_B = 0.81\overline{h}\omega$ and $E_{JT} > 3.0\overline{h}\omega$ for $h_B = 1.22\overline{h}\omega$. From these results, we can determine those portions of the curves plotted in figure 4 which are contributions from tunnelling.

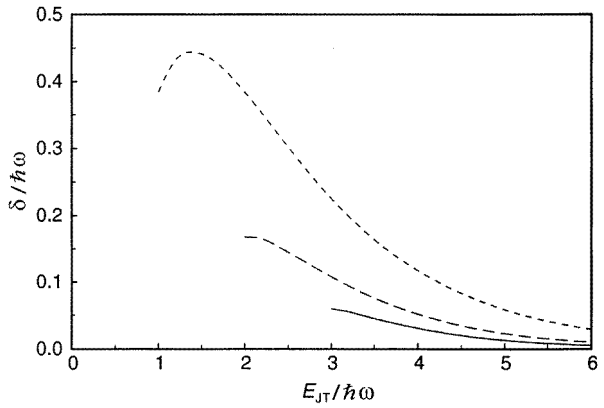

Figure 4. The inversion splitting as a function of E_{JT} for $h_B = 1.22\overline{h}\omega$ (solid line), $0.81\overline{h}\omega$ (long-dashed line) and $0.40\overline{h}\omega$ (short-dashed line). The separation between the minima is $d_M = \sqrt{\frac{8}{5}}|V_1|/\mu\omega^2$.

6. Conclusion

The $T_{1u} \otimes h_g$ JT system has been modelled including anisotropy for the first time. The ranges of values of the quadratic coupling constants for which minima of different types are formed have been clearly identified (in contrast to the case in which the second-order coupling terms are ignored, when there is a trough of minimum energy). New vibrational frequencies for the lower-symmetry local modes at the anisotropic minima have been calculated using the method of Öpik and Pryce [12]. A scale transformation procedure was then applied in order to incorporate the anisotropic frequencies automatically into the vibronic states corresponding to the pentagonal minima. It was shown that the new results correctly predict that the frequency of one of the e-modes tends to zero in the limit of linear coupling. The inversion splitting δ due to the tunnelling between the D_{5d} wells was calculated. As anisotropy affects the overlaps between the vibrational states localized in different minima, it has a dramatic effect on the magnitude of δ.

The scale transformation method has not yet been applied to the trigonal wells on account of difficulties introduced by virtue of the repeating IRs of the vibrational modes. However, it is hoped that it will be possible to extend the method to the D_{3d} wells in the near future. Also, it was not possible to apply the scale transformation at the initial stage of the problem (as was done in $T \otimes t$) in order to obtain expressions for the local frequencies for all coupling strengths. This is because in this case it is necessary to include quadratic coupling in order to generate wells, which in turn results in equations which cannot be solved. However, strong-coupling results have been obtained for the D_{3d} wells.

Acknowledgments

The authors would like to thank Dr M C M O'Brien and Dr C C Chancey for many valuable and helpful discussions on JT effects in icosahedral systems. This work has been made possible through the award of a NATO grant. One of us (YML) also wishes to thank the University of Nottingham for a Research Fellowship.

Appendix. Details of the derivation of the S matrices for the scale transformation at D_{5d} minima

As the ground electronic states at the D_{5d} minima transform as the irreducible representation A_{2u} of the point group D_{5d}, the symmetry operations which do not change the ground electronic states (apart from a possible change in its sign) must also belong to the D_{5d} group. In well A, for example, these symmetry rotations are

$$\{E\}, \{C_5^A, \bar{C}_5^A\}, \{C_5^{A,2}, \bar{C}_5^{A,2}\}, \{C_2^{\bar{B}D}, C_2^{\bar{F}C}, C_2^{E\bar{F}}, C_2^{BC}, C_2^{DE}\} \tag{A.1}$$

where $\bar{A}$, $\bar{B}$, $\bar{C}$, etc denote the inverse states. As the ground electronic states at the D_{5d} minima correspond to corners of an icosahedron, the meanings of the above symmetry operations can be illustrated as shown in figure A1. For example, C_5^A represents a symmetry rotation by $2\pi/5$ about the $\bar{A}A$ axis in an anticlockwise direction. Those operations with a bar over C are clockwise rotations. The matrix forms of these symmetry rotation operators are reducible within the bases

$$|\phi_1\rangle = |\theta\rangle \qquad |\phi_2\rangle = |\epsilon\rangle \qquad |\phi_3\rangle = |4\rangle \qquad |\phi_4\rangle = |5\rangle \qquad |\phi_5\rangle = |6\rangle. \tag{A.2}$$

The reduction of these matrices into IRs of D_{5d} is equivalent to finding new combinations

$$|\psi_{\nu m}\rangle = \sum_i S_{\nu m,i} |\phi_i\rangle \tag{A.3}$$

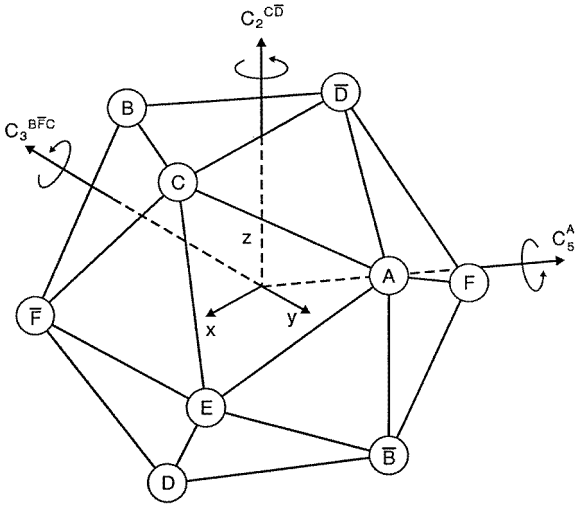

Figure A1. Labelling of the electronic states at D_{5d} minima and an illustration of the icosahedral rotation operators.

which transform as the IRs A_{1g}, E_{1g} and E_{2g} of the D_{5d} group. Thus the required combination of coefficients satisfies the eigen-equations [16]

$$\sum_j \left[\langle \phi_i | \begin{pmatrix} C \\ C(S) \end{pmatrix} | \phi_j \rangle - \begin{pmatrix} \nu \\ m \end{pmatrix} \delta_{ij} \right] S_{\nu m,j} = 0. \tag{A.4}$$

Here C and $C(S)$ are the class operators of the group chain $D_{5d} \supset D_{2d}$. For example, at well A we can choose the class operator $C = C_5^A + \bar{C}_5^A$ belonging to D_{5d} and the class operator $C(S) = C_2^{EF}$ belonging to D_{2d}. Then the S matrix can be constructed from

$$S = \begin{bmatrix} S_{\nu m,1} & S_{\nu m,2} & \dots & \dots \\ S_{\nu' m',1} & S_{\nu' m',2} & \dots & \dots \\ \dots & \dots & \dots & \dots \end{bmatrix}. \tag{A.5}$$

For the D_{5d} minima, the S matrices for all six wells are given by

$$S_A = \frac{1}{\sqrt{10}} \begin{bmatrix} -\sqrt{3} & -1 & \sqrt{6} & 0 & 0 \\ \phi^2 & -\sqrt{3}\phi^{-1} & \sqrt{2} & 0 & 0 \\ 0 & 0 & 0 & u & \phi u \\ \phi^{-2} & \sqrt{3}\phi & \sqrt{2} & 0 & 0 \\ 0 & 0 & 0 & -\phi u & u \end{bmatrix} \tag{A.6}$$

$$S_B = \frac{1}{\sqrt{10}} \begin{bmatrix} \sqrt{3} & 1 & \sqrt{6} & 0 & 0 \\ \phi^2 & -\sqrt{3}\phi^{-1} & -\sqrt{2} & 0 & 0 \\ 0 & 0 & 0 & u & -\phi u \\ \phi^{-2} & \sqrt{3}\phi & -\sqrt{2} & 0 & 0 \\ 0 & 0 & 0 & \phi u & u \end{bmatrix} \tag{A.7}$$

$$S_C = \frac{1}{\sqrt{10}} \begin{bmatrix} \sqrt{3} & -1 & 0 & \sqrt{6} & 0 \\ \phi^{-2} & -\sqrt{3}\phi & 0 & -\sqrt{2} & 0 \\ 0 & 0 & \phi u & 0 & u \\ \phi^2 & \sqrt{3}\phi^{-1} & 0 & -\sqrt{2} & 0 \\ 0 & 0 & u & 0 & -\phi u \end{bmatrix} \tag{A.8}$$

$$S_D = \frac{1}{\sqrt{10}} \begin{bmatrix} \sqrt{3} & -1 & 0 & -\sqrt{6} & 0 \\ \phi^{-2} & -\sqrt{3}\phi & 0 & \sqrt{2} & 0 \\ 0 & 0 & -\phi u & 0 & u \\ \phi^2 & \sqrt{3}\phi^{-1} & 0 & \sqrt{2} & 0 \\ 0 & 0 & u & 0 & \phi u \end{bmatrix} \tag{A.9}$$

$$S_E = \frac{1}{\sqrt{10}} \begin{bmatrix} 0 & 2 & 0 & 0 & \sqrt{6} \\ \sqrt{5} & \sqrt{3} & 0 & 0 & -\sqrt{2} \\ 0 & 0 & u & \phi u & 0 \\ \sqrt{5} & -\sqrt{3} & 0 & 0 & \sqrt{2} \\ 0 & 0 & -\phi u & u & 0 \end{bmatrix} \tag{A.10}$$

$$S_F = \frac{1}{\sqrt{10}} \begin{bmatrix} 0 & 2 & 0 & 0 & -\sqrt{6} \\ \sqrt{5} & \sqrt{3} & 0 & 0 & \sqrt{2} \\ 0 & 0 & u & -\phi u & 0 \\ \sqrt{5} & -\sqrt{3} & 0 & 0 & -\sqrt{2} \\ 0 & 0 & \phi u & u & 0 \end{bmatrix} \tag{A.11}$$

where

$$u = \sqrt{\frac{10}{\phi + 2}}.$$

References

[1] Khlopin V P, Polinger V Z and Bersuker I B 1978 *Theor. Chim. Acta* **48** 87–101
[2] Pooler D R 1980 *J. Phys. C: Solid State Phys.* **13** 1029–42
[3] Auerbach A, Manini N and Tosatti E 1994 *Phys. Rev.* B **49** 12 998–13 007
[4] O'Brien M C M 1996 *Phys. Rev.* B **53** 377–89
[5] Ceulemans A and Vanquickenborne L G 1989 *Struct. Bonding* **71** 125–59
[6] Dunn J L and Bates C A 1995 *Phys. Rev.* B **52** 5996–6005
[7] Wang C-L, Wang W-Z, Liu Y-L, Su Z-B and Yu L 1995 *Phys. Rev.* B **50** 5676–9
[8] Liu Y M, Polinger V Z, Bates C A and Dunn J L 1996 *J. Phys.: Condens. Matter* **8** L523–9
[9] Ham F S 1965 *Phys. Rev.* A **138** 1727–40
Ham F S 1968 *Phys. Rev.* A **166** 307–21
[10] Bates C A and Dunn J L 1989 *J. Phys.: Condens. Matter* **1** 2605–16
[11] Dunn J L and Bates C A 1989 *J. Phys.: Condens. Matter* **1** 2617–29
[12] Öpik U and Pryce M H L 1957 *Proc. R. Soc.* A **238** 425–47
[13] Fowler P W and Ceulemans A 1985 *Mol. Phys.* **54** 767–85
[14] Ceulemans A 1987 *J. Phys. Chem.* **87** 5374–85
[15] Dunn J L and Bates C A 1989 *J. Phys.: Condens. Matter* **1** 375–94
[16] Chen J-Q and Gao M-J 1992 *J. Math. Phys.* **23** 928–43